Molecular Immunology 116 (2019) 63–72

Contents lists available at ScienceDirect

Molecular Immunology

journal homepage: www.elsevier.com/locate/molimm

Splicing regulator SRSF1-3 that controls somatic hypermutation of IgV genes interacts with topoisomerase 1 and AID

Amit Kumar Singh[a], Anubhav Tamrakar[a], Ankit Jaiswal[a], Naoki Kanayama[b], Anshu Agarwal[c], Prabhanshu Tripathi[c], Prashant Kodgire[a,*]

[a] Discipline of Biosciences and Biomedical Engineering, Indian Institute of Technology Indore, Indore, 453 552, Madhya Pradesh, India
[b] Graduate School of Interdisciplinary Science and Engineering in Health Systems, Okayama University, Tsushima-Naka, Kita-Ku, Okayama 700-8530, Japan
[c] Translational Health Science, and Technological Institute, NCR Biotech Science Cluster, 3rd Milestone Gurugram-Faridabad Expressway, Faridabad, Haryana 121001, India

ARTICLE INFO

Keywords:
Activation-induced cytidine deaminase (AID)
Somatic hypermutation (SHM)
Immunoglobulin (*Ig*) genes
Splicing regulator SRSF1-3
Topoisomerase 1 (TOP1)

ABSTRACT

Somatic hypermutation (SHM) of *Ig* genes is initiated by activation-induced cytidine deaminase (AID) and requires target gene transcription. A splice isoform of SRSF1, SRSF1-3, is necessary for AID-dependent SHM of *Ig*V genes. Nevertheless, its exact molecular mechanism of action in SHM remains unknown. Our *in silico* studies show that, unlike SRSF1, SRSF1-3 lacks a strong nuclear localization domain. We show that the absence of RS domain in SRSF1-3 affects its nuclear localization, as compared to SRSF1. Consequently, SRSF1-3 is predominantly present in the cytoplasm. Remarkably, co-immunoprecipitation studies showed that SRSF1-3 interacts with Topoisomerase 1 (TOP1), a crucial regulator of SHM that assists in generating ssDNA for AID activity. Moreover, the immunofluorescence studies confirmed that SRSF1-3 and TOP1 are co-localized in the nucleus. Furthermore, Proximity Ligation Assay corroborated the direct interaction between SRSF1-3 and TOP1. An interaction between SRSF1-3 and TOP1 suggests that SRSF1-3 likely influences the TOP1 activity and consequently can aid in SHM. Accordingly, SRSF1-3 probably acts as a link between TOP1 and SHM, by spatially regulating TOP1 activity at the *Ig* locus. We also confirmed the interaction between SRSF1-3 and AID in chicken B-cells. Thus, SRSF1-3 shows dual-regulation of SHM, via interacting with AID as well as TOP1.

1. Introduction

The processes of somatic hypermutation (SHM) and class switch recombination (CSR) of immunoglobulin (*Ig*) genes are initiated by the activation-induced cytidine deaminase (AID). These processes are important for the generation of antibody repertoire, which ultimately assists in combating against a diverse range of pathogens. Thus, the absence of AID results in immunodeficiencies (Conley et al., 2009), but on the other hand, AID is a dangerous mutator. Numerous proto-oncogenes have been reported to be targeted by AID in B-cells (Pasqualucci et al., 2001; Shen et al., 1998). In fact, aberrant AID expression can lead to genomic instability, chromosomal translocation, even leading to tumorigenesis (Choudhary et al., 2018; Pasqualucci et al., 2008). The precise molecular mechanism by which AID targets *Ig* genes still remains enigmatic. Nevertheless, the process of SHM requires transcription initiation (Peters and Storb, 1996) as well as elongation (Kodgire et al., 2013).

Progression of the replication as well as transcription machinery on the DNA template generates negative and positive supercoiling, upstream as well as downstream of the replication fork and the transcription bubble, respectively (Yu and Droge, 2014). AID acts only on the ssDNA that is generated during the process of transcription (Wang et al., 2014). Typically, TOP1 relieves the supercoiling generated during transcription (Pommier, 2006). As expected, a decrease in the TOP1 levels increases SHM frequency in B-cells, and contrarily, overexpression of TOP1 suppresses SHM (Kobayashi et al., 2011). Consistently, TOP1 deficiency in knockdown cells leads to RNA polymerase II (RNA Pol II) accumulation and enhanced AID access to the *Ig* variable genes (Maul et al., 2015). However, spatial regulators of TOP1 at the *Ig* locus are not known yet.

AID has been reported to be linked with various proteins, including splicing-related factors, such as PTBP2 (Nowak et al., 2011) and

Abbreviations: AID, activation-inducedcytidine deaminase; CSR, classswitch recombination; Ig, immunoglobulin; Pol, RNApolymerase II; SHM, somatichypermutation; SRSF1, serine/arginine-richsplicing factor 1; SRSF1-3, serine/arginine-richsplicing factor 1-3; TOP1, topoisomerase1

* Corresponding author.
E-mail address: pkodgire@iiti.ac.in (P. Kodgire).

https://doi.org/10.1016/j.molimm.2019.10.002
Received 8 August 2019; Received in revised form 24 September 2019; Accepted 1 October 2019
Available online 15 October 2019
0161-5890/

CTNNBL1 (Conticello et al., 2008). Though, the role of these splicing factors in the directing AID to SHM targets and *Ig* diversification is largely unknown. A key splicing regulator called polypyrimidine tract binding protein-2 (PTBP2) acts as an AID interactor and enhances the binding of AID to switch region of DNA (Nowak et al., 2011). In fact, high-resolution confocal microscopy experiments with live cells expressing fluorescently tagged AID revealed that AID is localized to the sub-nuclear domains that are enriched in the splicing and RNA processing factors (Hu et al., 2014). Thus, changes in any of the spliceosome components might feasibly affect the targeting of AID. Indeed, a splice isoform of SR protein, serine/arginine-rich splicing factor 1 (SRSF1), SRSF1-3, is a key splicing regulator that is essential for the AID-dependent SHM apparatus to target the *Ig*V genes. SRSF1-3 is crucial for the AID-dependent SHM machinery by restoring and enhancing the hypermutation rate of *Ig*V genes in chicken B-cells (Kanehiro et al., 2012). Additionally, SRSF1-3 is also known to be involved in the buildup of AID inside the nucleus, and this accumulation is dependent on the AID C-terminal domain (Kawaguchi et al., 2017). However, the precise role of SRSF1-3 in SHM is yet largely unclear. In this study, we are interested to understand the molecular mechanism of an important splicing regulator, SRSF1-3, in SHM.

Here, we employed *in silico* studies and confocal microscopy techniques to study the subcellular localization of SRSF1-3, as well as performed co-immunoprecipitation, colocalization and PLA studies to identify and confirm the interacting partners of SRSF1-3 that may have a potential role in SHM of *Ig* genes.

2. Results

2.1. In silico studies for SRSF1 and SRSF1-3

SRSF1-3, a splice isoform of SR protein SRSF1, is essential for AID-dependent SHM of *Ig*V genes. Typically, the SR proteins have two distinct motifs, i.e., 1-2 RNA recognition motif (RRM), generally present at the N-terminus, and an RS domain consisting of multiple arginine and serine amino acids, at the C-terminus (Shepard and Hertel, 2009). Incidentally, the chicken SRSF1 locus codes for a 247 amino acid protein, which is involved in splicing, can also generate two splice variants namely SRSF1-2 and SRSF1-3 (previously known as ASF-2 and ASF-3, respectively) (Ge et al., 1991). The functions of these splice variants still remain enigmatic. We performed sequence alignments between chicken SRSF1 NCBI (NC_006106.3) and SRSF1-3 cDNA as well as protein sequences to find out the sequence and structural similarity between the splice variants (Fig. 1A). SRSF1 gene consists of four exons and codes for 2 RRM domains (17 – 91 and 121 – 195), and an RS domain (198 – 247) of which 78% amino acids are arginine and serine. Unlike SRSF1, its isoform SRSF1-3 lacks the exon 4 that codes for a small portion (11 amino acids; 185 – 195) of the RRM2 domain as well as an RS domain, instead the exon 3 is extended in the neighbouring intron that codes for a C-terminal domain and also bring a termination site. To understand differences in the C-terminal domain of SRSF1 and SRSF1-3, we performed sequence alignments between SRSF1 and SRSF1-3 proteins by using EMBOSS Needle (Fig. 1B). Both protein sequences are identical up to the E184 amino acid; however, amino acids sequence from 185 onwards is different between SRSF1 and SRSF1-3. Moreover, a new domain in the SRSF1-3 isoform in which the C-terminal RS domain is substituted consists of only 8 R + S amino acids, compared to 39 R + S amino acids in SRSF1 (Fig. 1C).

The RS domain of SRSF1 is supposed to be the main site for the post-translational modification, especially phosphorylation at the serine residues, and believed to play an important role in nucleo-cytoplasmic shuttling of SRSF1 and thereby regulate its sub-nuclear localization (Caceres et al., 1997). Thus, the absence of RS domain in SRSF1-3 is likely to impact on its nuclear localization. To confirm whether the lack of RS domain in SRSF1-3 has affected its nuclear localization signal (NLS), we performed NLS prediction with amino acid sequences by using a popular NLStradamus tool (Nguyen Nguyen Ba et al., 2009). NLS prediction of SRSF1 shows two potential NLSs at the spacer between RRM1 and RRM2 domains (96 to 112 amino acids) and at the RS domain (203 to 248 amino acids), respectively (Fig. 2). As expected, SRSF1-3 shows only one weak NLS at the spacer between RRM1 and RRM2 domains (96 to 111 amino acids) (Fig. 2), which is likely to affect its localization pattern.

2.2. The absence of RS domain in SRSF1-3 affects its nuclear localization

To confirm whether the absence of RS domain and lack of a strong NLS in SRSF1-3 have any effect on its nuclear localization, we expressed SRSF1-3 into chicken DT40-ASF cells. We used DT40-ASF chicken B-cell line in which both the endogenous SRSF1 genes are knocked out and a human SRSF1 cDNA was expressed (Wang et al., 1996). An expression vector of SRSF1-3 cDNA containing FLAG tag at its N-terminus (**Fig. S1**) was introduced into DT40-ASF cells to create the SRSF1-3 reconstituted clones. Two independent reconstituted clones (Clone no. 41 and 47) were confirmed for the expression of SRSF1-3 cDNA and SRSF1-3 protein by western blotting using the anti-FLAG antibody (**Fig. S2**).

To study the localization of FLAG-SRSF1-3 protein, we performed the high-resolution confocal microscopy studies using two independent reconstituted clones of SRSF1-3 and the SRSF1-3 deficient control cells. We checked localization of SRSF1 using the anti-SF2/ASF primary antibody and the anti-mouse secondary antibody tagged with fluorescent dye Alexa Fluor 488 (**Table S1**), in DT40 cells. Similarly, we checked

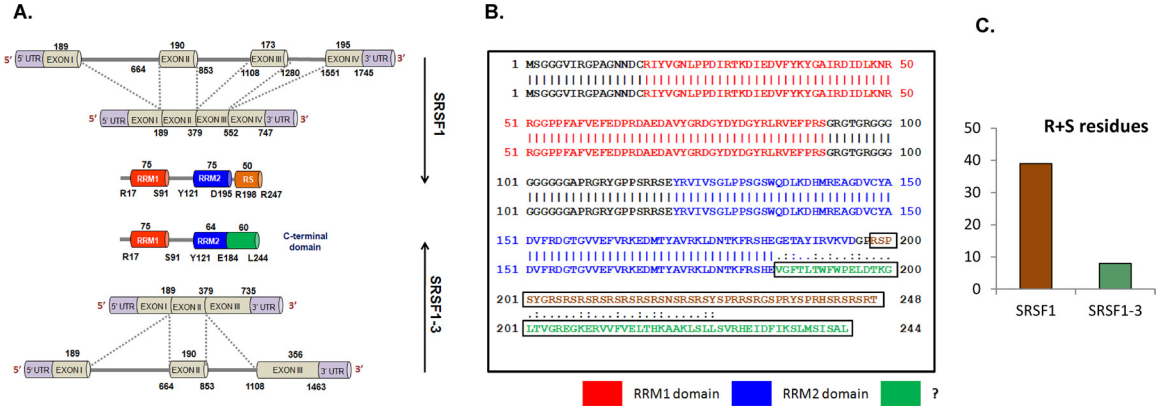

Fig. 1. *In silico* studies for SRSF1 and SRSF1-3. A. The schematic diagram of chicken SRSF1 and its splice variant SRSF1-3. RRM, RNA recognition motif; RS, serine/arginine-rich region. **B.** Protein sequence alignment between SRSF1 and SRSF1-3. Lines show identity, dots show similarity, and gaps represent not-identical and not-similar amino acid to each other. **C.** The histograms show the total number of serine and arginine amino acids in SRSF1 and SRSF1-3.

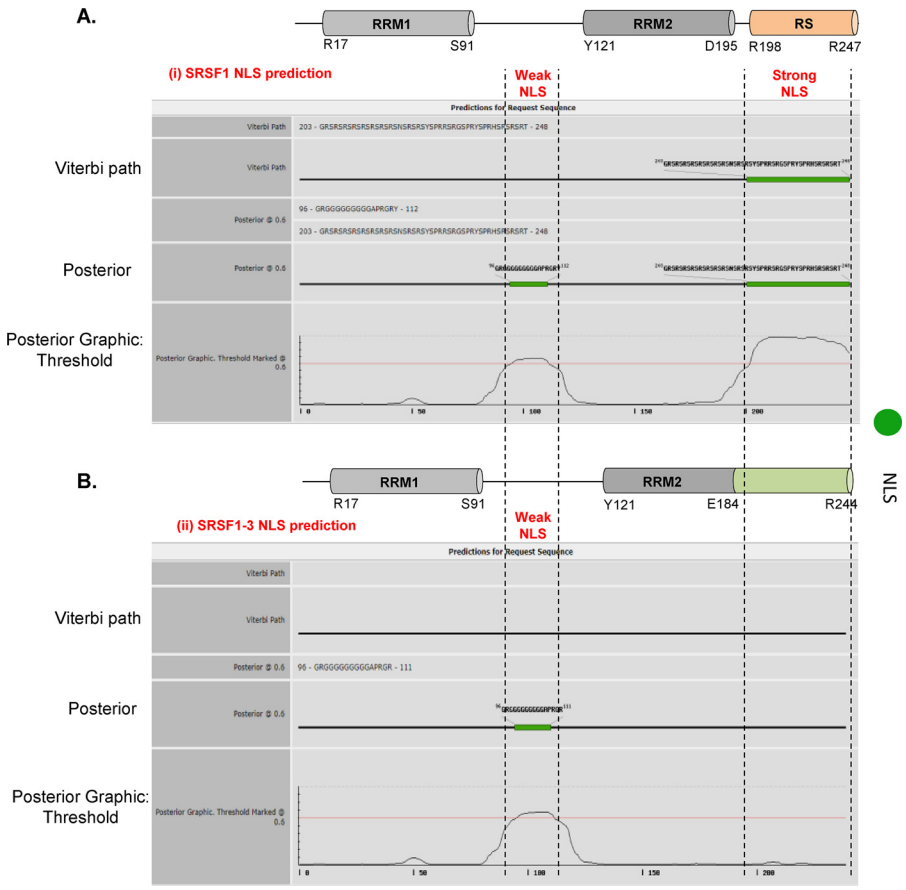

Fig. 2. Nuclear localization signal (NLS) prediction for amino acid sequences of SRSF1 and SRSF1-3 using NLStradamus (http://www.moseslab.csb.utoronto.ca/NLStradamus). (i) SRSF1 shows two potential NLS residues, the first between 96 to 112 aa in the spacer between two RRM domains, and the second between 203 to 248 aa at RS domain. (ii) SRSF1-3 shows only one weak NLS at 96 to 111 aa in the spacer between two RRM domains (For interpretation of the references to colour in this figure legend, the reader is referred to the web version of this article).

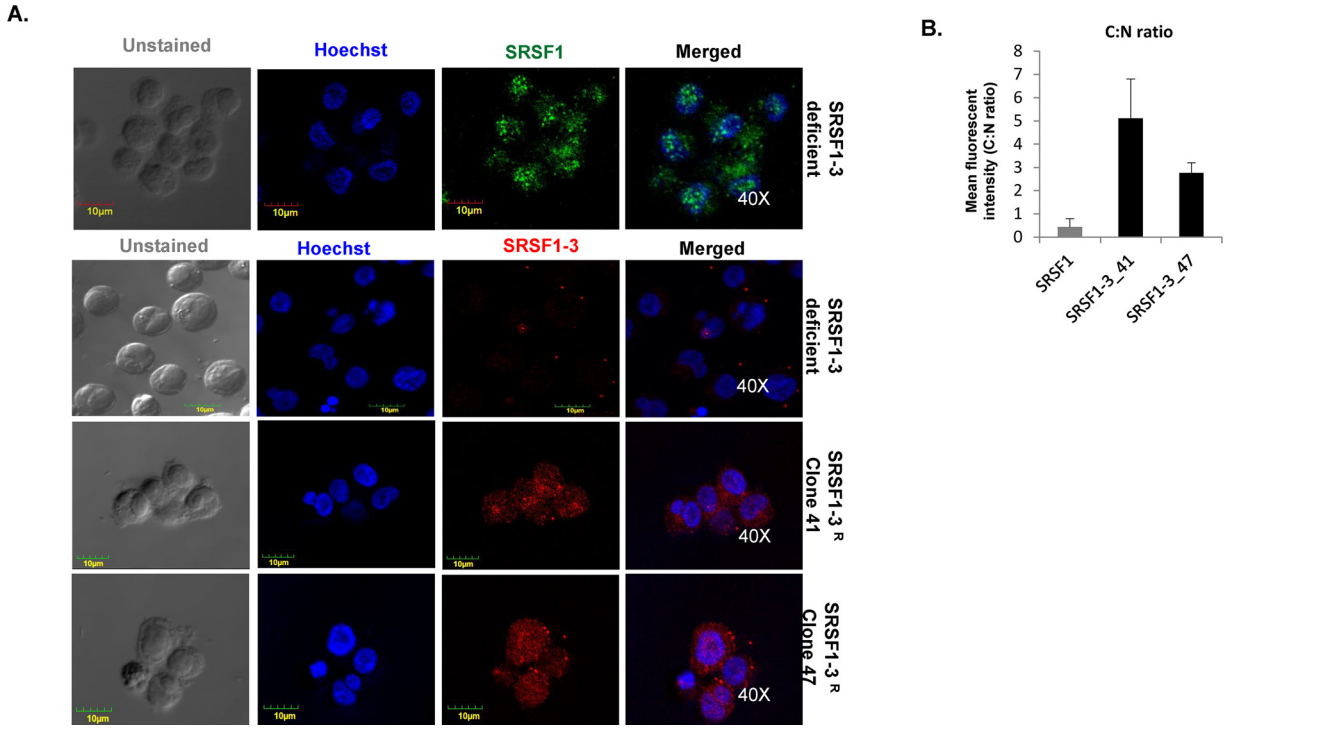

Fig. 3. The absence of RS-domain in SRSF1-3 affects its nuclear localization. A. The localization of SRSF1 and SRSF1-3 in chicken DT40 SRSF1-3 reconstituted clones and the SRSF1-3 deficient cells were observed by confocal microscopy. Images were taken at 40X magnification. Panel 1 and 2 is for DT40-ASF SRSF1-3 deficient cells stained with the anti-SRSF1 and anti-FLAG antibodies, respectively; Panel 3 and 4 is for SRSF1-3 reconstituted clones stained with the anti-FLAG antibody **B.** The mean fluorescent intensities of nuclear and cytoplasmic SRSF1 and SRSF1-3 were quantitated using the ImageJ processing program. The histograms represent cytoplasm: nucleus (C:N) ratios of SRSF1 and SRSF1-3. (For interpretation of the references to colour in this figure legend, the reader is referred to the web version of this article).

localization of FLAG-SRSF1-3 using the anti-FLAG mAB primary antibody and the anti-mouse secondary antibody tagged with fluorescent dye Alexa Fluor 594 (**Table S1**), in the SRSF1-3 deficient and two independent SRSF1-3 reconstituted clones. As expected, we observed SRSF1 was predominantly localized in the nucleus (Fig. 3A, panel 1), as it contains a strong NLS in the RS domain. However, we observed the localization of the FLAG-SRSF1-3 protein, in both the SRSF1-3 reconstituted clones, largely in the cytoplasm (Fig. 3A, panel 2-4). To calculate C:N ratios of SRSF1 and SRSF1-3, we compared the mean fluorescent intensities of SRSF1 and SFSR1-3 in cytoplasm and nucleus. The calculated mean fluorescent intensity confirmed that the localization of SRSF1 was more inside the nucleus than the cytoplasm, whereas, SRSF1-3 is more abundant in the cytoplasm than in the nucleus (Fig. 3B). Thus, we conclude that the absence of RS domain and lack of a strong NLS in SRSF1-3 affects its nuclear localization.

2.3. Interaction of SRSF1-3 with TOP1 and AID influencing IgV diversification

Subsequent to its nuclear localization, SRSF1-3 may interact with other proteins and thus regulate various cellular functions. To identify interacting partners of SRSF1-3, we performed co-immunoprecipitation studies for the FLAG-tagged SRSF1-3 using anti-FLAG antibody, in SRSF1-3 reconstituted clones, and compared with the SRSF1-3 deficient control cells. Co-immunoprecipitation studies using anti-SRSF1-3-FLAG showed numerous interacting partners of SRSF1-3 (Fig. 4, lane 2 and 3), as compared to the SRSF1-3 deficient cells (Fig. 4, lane 1). These results suggest that the splicing regulator SRSF1-3 is networking with several proteins, and thus can influence various important cellular functions via multiple interacting partners. Interestingly, we observed a distinct band at 90 kDa in the immunoprecipitated samples of SRSF1-3 reconstituted clones, similar to the size of Topoisomerase 1 (TOP1). We confirmed that SRSF1-3 interacts with TOP1 by performing western blotting using the anti-TOP1 antibody (**Table S1**), which shows a specific band at 90 kDa in SRSF1-3 reconstituted cells and is missing in the SRSF1-3 deficient cells (Fig. 5A**, S**3A). We further confirmed this interaction by performing co-immunoprecipitation using the anti-TOP1 antibody and detected SRSF1-3-FLAG bands using the anti-FLAG antibody (**Table S1**) in the SRSF1-3 reconstituted cells, as compared with the SRSF1-3 deficient cells (Fig. 5B**, S3B**), confirming an interaction of SRSF1-3 with TOP1, which probably influences the SHM of *Ig* genes. Since the SRSF1-3 deficient control cells do not contain FLAG-tagged SRSF1-3, the input samples do not show any band for SRSF1-3 (Fig. 5B, panel 1).

To confirm the interaction of SRSF1-3 and TOP1 in the nucleus and to exclude the possibility that binding of SRSF1-3 to TOP1 is the result of an artificial interaction by mixing proteins from cytoplasm and nuclei during the preparation of cell lysate, we performed co-immunoprecipitation of SRFS1-3 from nuclear extracts by using the anti-FLAG antibody and western blotting by using the anti-TOP1 antibody (**Table S1**). To confirm purity of nuclear extract, we performed immunoblotting using cytoplasm specific (GAPDH) and nucleus specific (Histone H3) antibodies (**Table S1**). As expected, we observed Histone H3 bands in the nuclear extract and GAPDH was absent in the nuclear extract, confirming purity of the nuclear extract (Fig. 5**C and S3C**). Immunoprecipitation of SRFS1-3 from nuclear extracts by using the anti-FLAG antibody also shows a specific band at 90 kDa in SRSF1-3 reconstituted cells and is missing in the SRSF1-3 deficient cells (Fig. 5**D and S3D**). These results are identical to co-immunoprecipitation experiments with the whole cell lysates, confirming that SRSF1-3 and TOP1 interact in the nucleus. Similarly, we further confirmed this interaction by performing co-immunoprecipitation of TOP1 from the nuclear extracts by using the anti-TOP1 antibody and detected SRSF1-3-FLAG bands using the anti-FLAG antibody (**Table S1**) in the SRSF1-3 reconstituted cells, as compared with the SRSF1-3 deficient cells (Fig. 5**E and S3E**), confirming an interaction of SRSF1-3 with TOP1 in the nucleus, which probably influences the SHM of *Ig* genes. Since the SRSF1-3 deficient control cells do not contain FLAG-tagged SRSF1-3, the input samples do not show any band for SRSF1-3 (Fig. 5B, **5E** panel 1).

To confirm the earlier reports of interaction between SRSF1-3 and AID in human 293 T cells (Kawaguchi et al., 2017), we performed co-immunoprecipitation using the anti-FLAG antibody and detected AID by western blotting using the anti-AID antibody (**Table S1**), which shows a specific band at 24 kDa in SRSF1-3 reconstituted cells and is missing in the SRSF1-3 deficient cells (Fig. 5**F and S4A**). Subsequently, we confirmed this interaction by performing co-immunoprecipitation using the anti-AID antibody and detected SRSF1-3-FLAG bands using the anti-FLAG antibody (**Table S1**) in the reconstituted cells, as

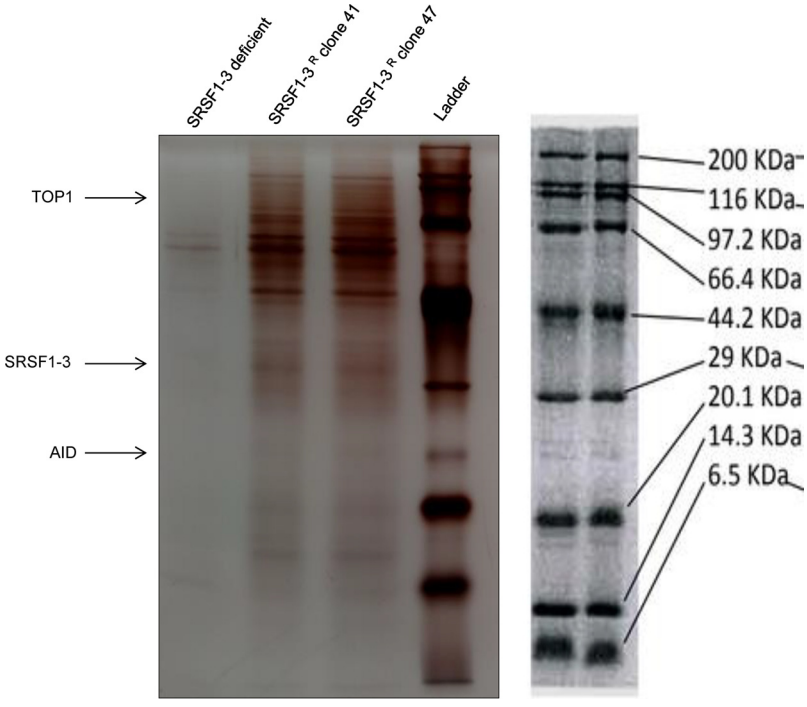

Fig. 4. Co-immunoprecipitation of FLAG-tagged SRSF1-3 in DT40-ASF cells Co-immunoprecipitation of FLAG-tagged SRSF1-3 reconstituted clones and the SRSF1-3 deficient control cells performed using the anti-FLAG magnetic beads, protein samples were run on 12% SDS-PAGE and analyzed by silver staining. Protein bands which match with the molecular weight of TOP1, AID and SRSF1-3 are shown by arrows.

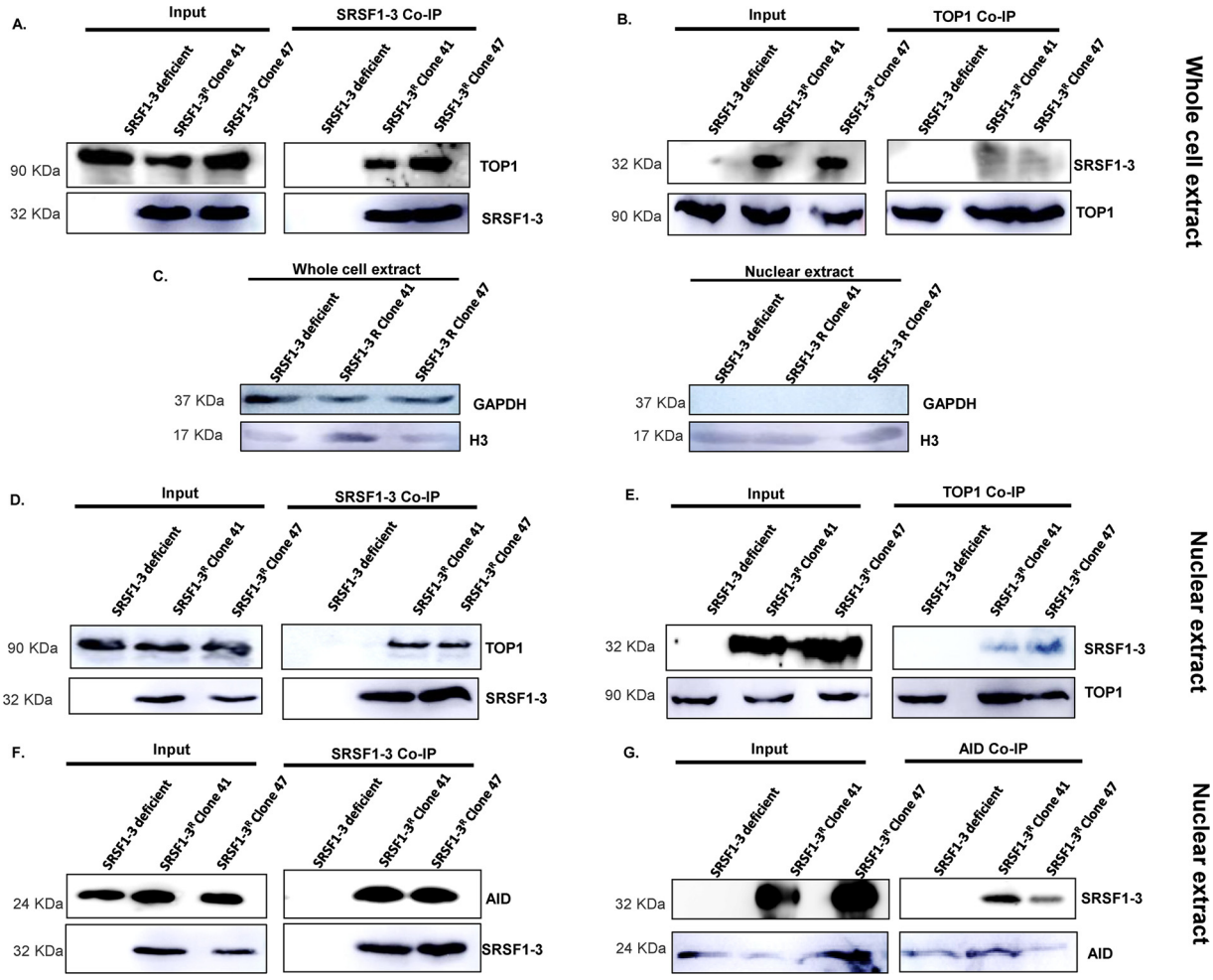

Fig. 5. SRSF1-3 interactions with TOP1 and AID in SRSF1-3 reconstituted clones and the SRSF1-3 deficient control cells: A. Co-immunoprecipitation of FLAG-tagged SRSF1-3 from the whole cell lysate performed using the anti-FLAG magnetic beads and analyzed by western blotting using the anti-TOP1 pAb and anti-FLAG mAb. **B.** Co-immunoprecipitation of TOP1 from the whole cell lysate performed using the anti-TOP1 pAb and protein-A agarose beads and analyzed by western blotting using the anti-FLAG mAb and anti-TOP1 pAb. **C.** The whole cell extract and nuclear extract fractions of the SRSF1-3 reconstituted cells and SRSF1-3 deficient cells were analyzed by western blotting using anti-GAPDH mAb and anti-Histone H3 mAb. GAPDH and Histone H3 were used as an internal control for the whole cell extract and nuclear extract fractions, respectively. **D.** Co-immunoprecipitation of FLAG-tagged SRSF1-3 from the nuclear extracts and performed using the anti-FLAG magnetic beads and analyzed by western blotting using the anti-TOP1 pAb and anti-FLAG mAb. **E.** Co-immunoprecipitation of TOP1 from the nuclear extracts and performed using the anti-TOP1 pAb and protein-A agarose beads and analyzed by western blotting using the anti-FLAG mAb and anti-TOP1 pAb. **F.** Co-immunoprecipitation of FLAG-tagged SRSF1-3 from whole cell lysate and performed using the anti-FLAG magnetic beads and analyzed by western blotting using the anti-AID mAb and anti-FLAG mAb. **G.** Co-immunoprecipitation of AID from whole cell lysate and performed using the anti-AID mAb and protein-A agarose beads and analyzed by western blotting using the anti-FLAG mAb and anti-AID mAb. (Full gel image for Fig. 5 A-E is in Supplementary Figure S3 and full gel image for Fig. 5 F-G is in Supplementary Figure S4).

compared with the SRSF1-3 deficient cells (Fig. 5**G and S4B**), confirming an interaction of SRSF1-3 with AID, which probably influences the SHM of *Ig* genes. Since the SRSF1-3 deficient control cells do not contain FLAG-tagged SRSF1-3, the input samples do not show any band for SRSF1-3 (Fig. 5G, panel 1). These results suggest that SRSF1-3 interacts with AID and another crucial regulator of SHM, TOP1, and thus influences the process of SHM.

Several commercial AID antibodies tend to be non-specific, and therefore can show multiple off-target bands by western blotting. To confirm that the pulldown band is specific, we performed western blotting using the anti-AID antibody (**Table S1**) for the negative controls (DT40 AID$^{-/-}$) as well as for the SRSF1-3 reconstituted cells and the SRSF1-3 deficient cells. We observed a specific band at 24 kDa in SRSF1-3 reconstituted cells and the SRSF1-3 deficient cells, which is missing in DT40 AID$^{-/-}$, the negative control cells (**Fig. S**5A). Moreover, there were no background bands in SRSF1-3 reconstituted cells and the SRSF1-3 deficient cells, confirming the specificity of the pulldown bands.

To confirm these interactions between SRSF1-3 and AID are different from the main transcript SRSF1, we performed co-immunoprecipitation using the anti-ASF antibody, which picks up both SRSF1 as well as SRSF1-3 and detected AID by western blotting using the anti-AID antibody (**Table S1**). We observed a specific band at 24 kDa for AID in SRSF1-3 reconstituted cells (**Fig. S6**), as the anti-ASF antibody picks up both SRSF1 as well as SRSF1-3. As expected, the specific AID band is missing in the SRSF1-3 deficient cells (**Fig. S6**), confirming that the interaction between SRSF1-3 and AID is different from the main transcript SRSF1.

2.4. Colocalization and proximity ligation assay (PLA) reveal the direct interaction between SRSF1-3 and TOP1

To validate our finding in the immunoprecipitation experiments about the interaction between SRSF1-3 and TOP1, we observed colocalization of these two proteins using double-immunofluorescence staining with polyclonal anti-TOP1 and monoclonal anti-FLAG

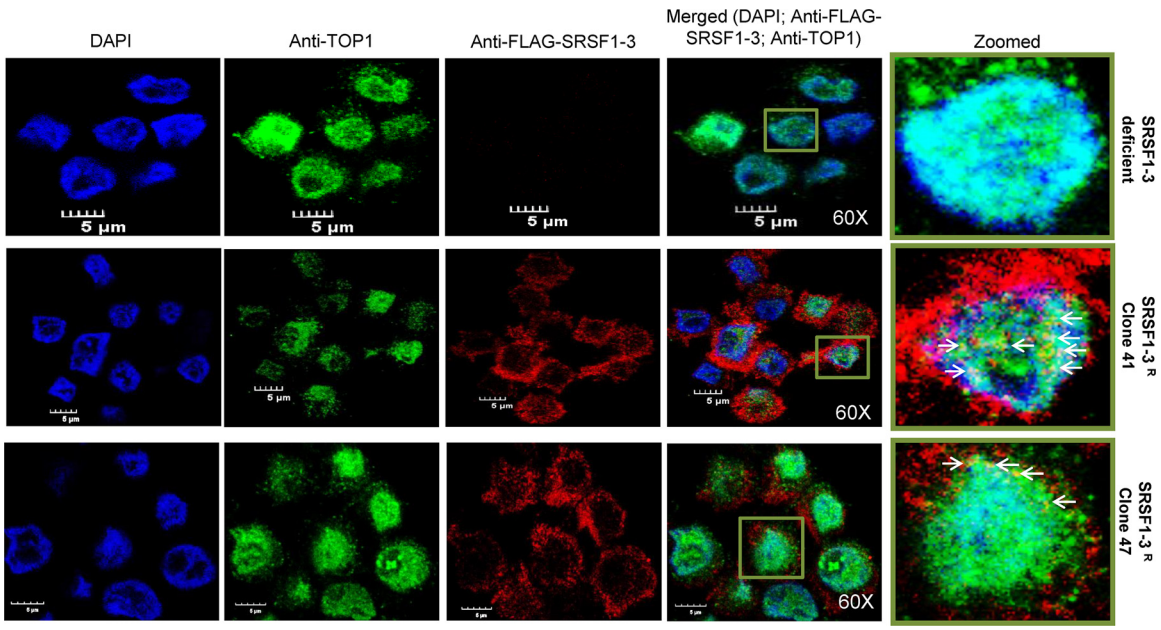

Fig. 6. Colocalization of SRSF1-3 and TOP1: DT40 SRSF1-3 reconstituted and the SRSF1-3 deficient control cells were fixed and subjected to double-immunofluorescence staining with polyclonal anti-TOP1 (green stained), and monoclonal anti-FLAG (red stained) antibodies. TOP1 is predominantly localized in the nucleus, overlapping DAPI (blue), whereas SRSF1-3 is mostly localized in the cytoplasm. Nuclei were counterstained with DAPI (blue). Yellow and orange signals that coincide with TOP1 and SRSF1-3 colocalization are marked with arrows in the zoomed images. (An enlarged image for Fig. 6 is in Supplementary Figure S7) (For interpretation of the references to colour in this figure legend, the reader is referred to the web version of this article).

antibodies (**Table S1**). As expected, due to the presence of strong NLS, TOP1 protein was observed exclusively in the nucleus, showing an overlapping signal with the DAPI stained nucleus (Fig. 6**, S7, S8** and **S9**). Similar to the earlier immunofluorescence straining experiments (Fig. 3), SRSF1-3 was predominantly present in the cytoplasm and only a small portion of SRSF1-3 was localized in the nucleus. Nevertheless, we observed several spots in yellow and orange, in the nucleus, which indicate TOP1 and SRSF1-3 colocalization in both SRSF1-3 reconstituted clones (Fig. 6**, S8** and **S9, panel 2 and 3**), confirming the earlier observations in the immunoprecipitation experiments that SRSF1-3 and TOP1 are present in a complex and likely to interact with each other. As expected, we did not observe such colocalization signals in the SRSF1-3 deficient control cells (Fig. 6**, S8** and **S9, panel 1**).

Furthermore, to ascertain molecular interactions between SRSF1-3 and TOP1, we performed Proximity Ligation Assay (PLA) studies, using Duolink kit. DT40 SRSF1-3 reconstituted cells and the SRSF1-3 deficient control cells were fixed and incubated with polyclonal anti-TOP1 and monoclonal anti-FLAG antibodies (**Table S1**), followed by incubation with secondary antibodies conjugated to oligonucleotides. We observed PLA signal (red spots) in the DT40 SRSF1-3 reconstituted cells (Fig. 7**, S12** and **S13, panel 2 and 3**), suggesting a direct interaction and proximity between SRSF1-3 and TOP1. For most of the cells we observed PLA signals in the nucleus, although rarely, some of the PLA spots were present in the cytoplasm as well, suggesting a direct interaction between TOP1 and SRSF1-3. In contrast, as expected, we did not observe any PLA signal in the SRSF1-3 deficient control cells (Fig. 7, **S12** and **S13, panel 1**)t-test and P-values are reported in figure legends. We observed 7.2% (P-value = 0.006) and 11.5% (P-value = 0.011) cells were showing positive PLA signal for the SRSF1-3 reconstituted clone 41 (**Fig. S10** and **S11**), which is statistically significant. Similarly, we observed 8.2% (P-value = 0.004) and 9.9% (P-value = 0.023) cells were showing positive PLA signal for the SRSF1-3 reconstituted clone 47 (**Fig. S10** and **S11**), which is statistically significant. Thus, the co-localization and PLA studies further validate our observations in the co-immunoprecipitation experiments, confirming an interaction between SRSF1-3 and TOP1.

In fact, interactions of TOP1 and SRSF1 (product of the main transcript) are reported earlier in which TOP1 structurally makes a complex with SRSF1, and phosphorylates the RS domain of SRSF1. The spacer region between the two RRM domains of SRSF1 influences the DNA nicking property of TOP1 which is essential for relaxation of DNA negative supercoiling (Ishikawa et al., 2012). *In silico* analysis of SRSF1 and SRSF1-3 shows substitution of the C-terminal RS domain, whereas the RRM1, RRM2, and the spacer regions are retained unaltered. Thus, SRSF1-3 is also likely to interact with TOP1. Our immunoprecipitation studies confirmed the interaction between SRSF1-3 and TOP1. (Fig. 5**A** and **5B**). Furthermore, the co-localization studies (Fig. 6**, S7, S8** and **S9**) and proximity ligation assay experiments (Fig. 7**, S10, S11, S12** and **S13**) corroborate the direct interaction between SRSF1-3 and TOP1. Generally, during the course of transcription, excessive negative supercoiling is introduced just upstream of the progressing transcription bubble, which is resolved by TOP1 via nicking (Baranello et al., 2013; Leppard and Champoux, 2005; Pommier, 2006). Thus, whenever transcription rates exceed the maximum TOP1 activity, non-B DNA structures tend to form due to unresolved negative supercoiling (Zhao et al., 2010). TOP1 activity at the *Ig* locus plays an important role in providing ssDNA substrate to AID and thus controls SHM (Maul et al., 2015). Remarkably, SRSF1 is known to interact with TOP1 (Ishikawa et al., 2012) and inhibit DNA cleavage by TOP1 (Kowalska-Loth et al., 2002). Similarly, SRSF1-3 is likely to interact with TOP1 and interferes with the DNA cleavage activity of TOP1. Thus, TOP1 could serve as a link between SRSF1-3 and SHM.

In summary, due to the absence of a strong nuclear localization signal located in the RS domain, SRSF1-3 is predominantly retained in the cytoplasm. Nevertheless, a portion of SRSF1-3 is localized in the nucleus since it contains a weak nuclear localization signal that is present between two RRM domains. After entering in the nucleus, it can locally interact with a vital regulator of SHM, TOP1, and likely inhibits its DNA cleavage activity to generate more ssDNA substrate for AID, and thus can enhance SHM. Additionally, SRSF1-3 interacts with AID protein, as reported in the earlier reports (Kawaguchi et al., 2017). Thus, SRSF1-3 demonstrates a dual role in SHM of *Ig* genes, via its interactions with a crucial regulator of SHM, TOP1, as well as AID (Fig. 8).

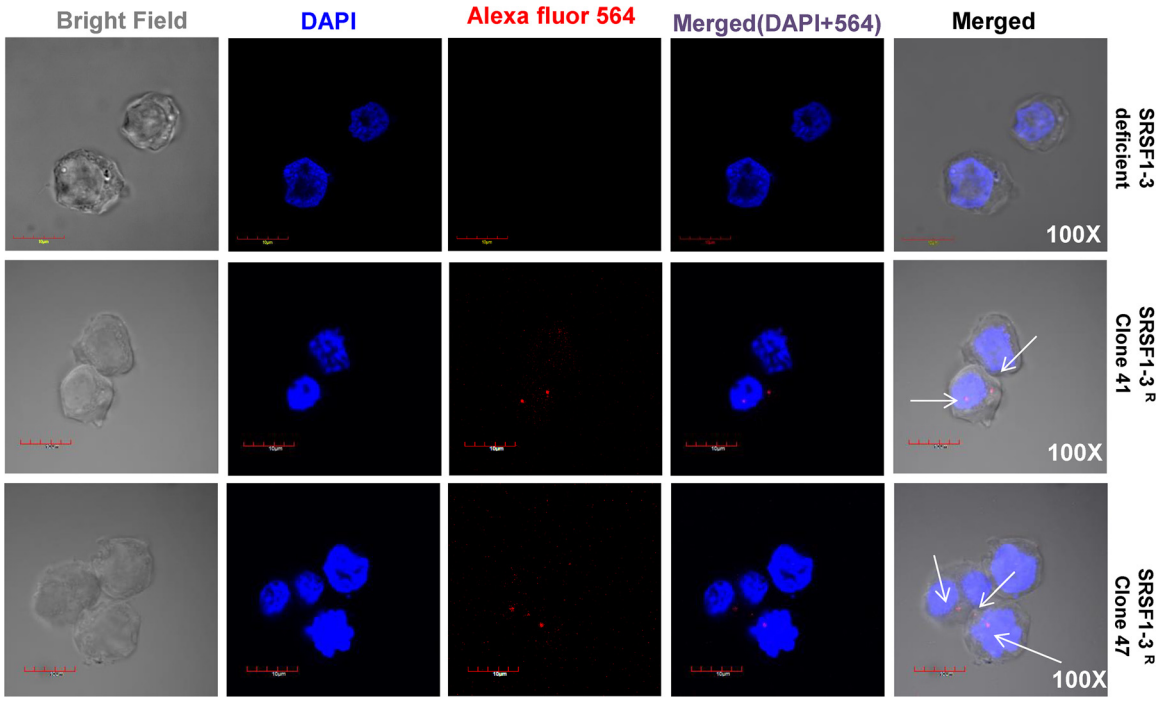

Fig. 7. Proximity Ligation Assay for SRSF1-3 and TOP1: Images demonstrate the PLA signals in DT40 chicken B-cells and the proximity between two proteins, SRSF1-3 and TOP1. Nuclei were stained with DAPI. FLAG-tagged SRSF1-3 and TOP1 were incubated with primary antibodies (Table S1), followed by incubation with secondary antibodies conjugated to oligonucleotides (PLA Probes anti-mouse MINUS and PLA Probes anti-rabbit PLUS). Each picture is representative of a typical cell staining observed in more than 10 fields randomly chosen. The top panel is for the SRSF1-3 deficient cells and the next two panels are for SRSF1-3 reconstituted clones. The red PLA spots in SRSF1-3 reconstituted clones are shown by arrows (For interpretation of the references to colour in this figure legend, the reader is referred to the web version of this article).

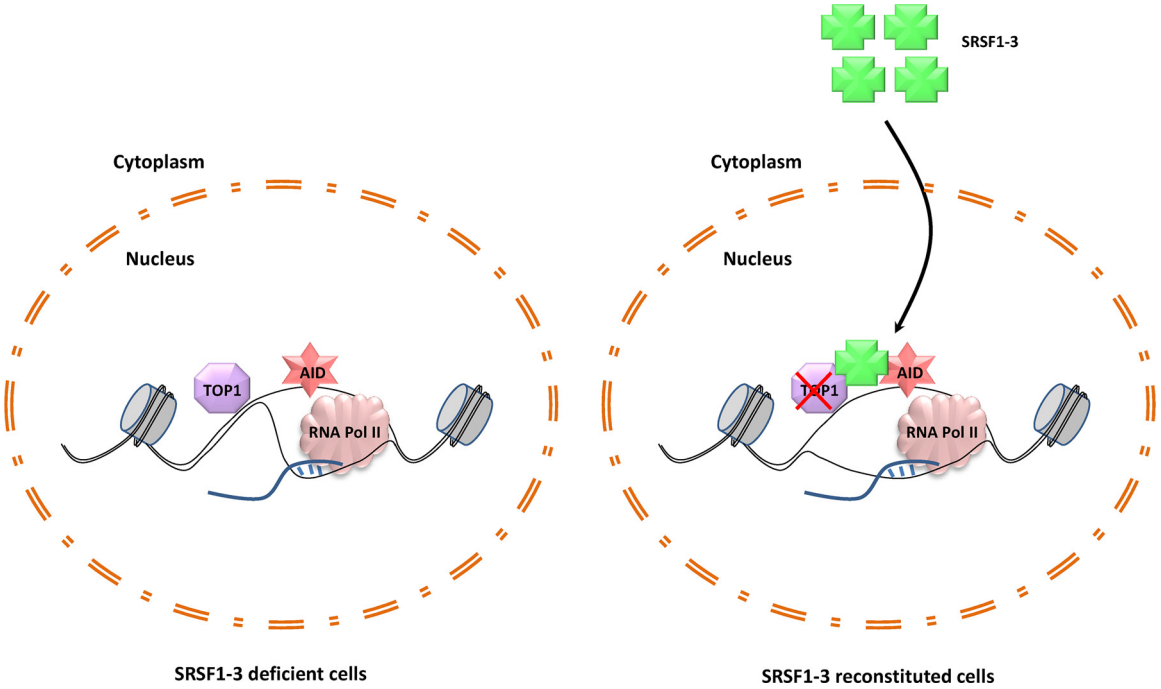

Fig. 8. Molecular mechanism of SRSF1-3 in SHM. Nuclear localization studies demonstrated that SRSF1-3 is predominantly localized in the cytoplasm, due to lack of RS domain. Once it enters in the nucleus, as confirmed by co-immunoprecipitation studies, SRSF1-3 interact with TOP1 as well as AID in chicken B-cells, and thus reveals direct regulation of somatic hypermutation by SRSF1-3. In the absence of SRSF1-3, TOP1 activity is unaltered leading to normal processing of negative supercoils and therefore reduced ssDNA substrate available for AID activity. However, the presence of SRSF1-3 affects TOP1 activity, leading to an abundance of ssDNA substrate for AID deamination (For interpretation of the references to colour in this figure legend, the reader is referred to the web version of this article).

3. Discussion

A diverse antibody repertoire is generated by a cumulative outcome of V(D)J recombination that is mediated by the RAG1/2 recombinase in bone marrow, followed by SHM and CSR in the secondary lymphoid organs, which ultimately leads to the generation of different classes of high-affinity antibodies. To meet the enormous cellular demands of antibodies, *Ig* locus is governed by a strong promoter. Thus, *Ig* locus is transcriptionally very active. SHM is initiated by AID that acts on the ssDNA substrate and deaminates cytidine to uridine (Choudhary et al., 2018; Pasqualucci et al., 2008). In addition to AID, SHM requires that the target genes are transcribed (Peters and Storb, 1996). During transcription and RNA Pol II possession, positive supercoiling is generated downstream and negative supercoiling is generated upstream of the transcription assembly, which is resolved by the TOP1 activity (Baranello et al., 2016). The negative supercoiling provides necessary ssDNA substrate for AID activity, whereas TOP1 activity has a negative impact on AID-dependent SHM. Consistently, the decrease in TOP1 leads to increase in AID-dependent SHM (Kobayashi et al., 2011).

The high-resolution confocal microscopy studies with live cells expressing fluorescently tagged AID revealed that AID is localized to the sub-nuclear domains that are enriched in the splicing factors (Hu et al., 2014). In fact, AID has been reported to be linked with various splicing-related factors, such as PTBP2 (Nowak et al., 2011) and CTNNBL1 (Conticello et al., 2008), in addition to SRSF1-3 (Kanehiro et al., 2012), a splice isoform of SRSF1. However, the precise role of these factors in the targeting of AID and *Ig* diversification is largely unclear. SRSF1-3, a key splicing regulator, is necessary for the AID-dependent SHM apparatus to target the *Ig*V genes. SRSF1-3, but not SRSF1, is targeted on the *Ig*V genes and is crucial for the AID-dependent SHM machinery by restoring and enhancing the hypermutation rate of *Ig*V genes in SRSF1-3 deficient chicken B-cells (Kanehiro et al., 2012). Moreover, SRSF1-3 is also reported to be involved in the accumulation of AID inside the nucleus which is dependent on the AID C-terminal domain (Kawaguchi et al., 2017).

Members of the family of serine/arginine (SR)-rich proteins play a crucial role in carrying out the essential processing of pre-mRNAs. There are 12 types of known SR proteins, which consist of at least one RRM domain and RS domain each. Incidentally, SRSF1 consists of two RRM domains and a single RS domain (Hagopian et al., 2008). SRSF1-3 is a splice isoform of SRSF1, and share an identical N-terminal region containing two RRM domains. However, the C-terminal RS domain that is rich in serine and arginine amino acids in SRSF1, is substituted in the splice variant SRSF1-3 with an extended exon 3, that now codes for a fewer serine and arginine amino acids. Interestingly, earlier studies reported that deletion of the RS domain in SRSF1 retains the splicing activity, suggesting that the RS domain is not required for its splicing activity (Caceres and Krainer, 1993; Caceres et al., 1997; Zhu and Krainer, 2000; Zuo and Manley, 1993). In fact, the RS domain is supposed to be the main site for the post-translational modification, especially phosphorylation at the serine residues by protein kinase SRPK, and play an important role in nucleo-cytoplasmic shuttling of SRSF1 and thereby regulate its sub-nuclear localization (Caceres et al., 1997). Incidentally, SRSF1-3 contains only 5 serine residues in its C-terminal domain, as compared to 20 serine residues in SRSF1 (Fig. 1).

AID is predominantly localized in the cytoplasm; however, co-expression of AID along with SRSF1-3 led to the higher nuclear accumulation of both AID as well as SRSF1-3. Nevertheless, SRSF1-3 is not essential for nuclear import of AID (Kawaguchi et al., 2017). Our *in silico* studies demonstrated that SRSF1-3 contains a weak nuclear localization signal (NLS) between 96 – 112 amino acids and lacks the strong NLS present in the RS domain of SRSF1 (Fig. 2). Indeed, it is predominantly present in the cytoplasm, as compared to SRSF1 (Fig. 3**A** and **B**). It seems the weak NLS present between the two RRM domains of SRSF1-3 could still assist in the higher nuclear accumulation of AID.

Niu et. al., hypothesized that genes with introns will recruit the spliceosome complex which helps in sequestering TOP1, whereas, in the intronless genes, TOP1 retains its activity and resolves negative supercoiling (Niu and Yang, 2011). Furthermore, it is reported that a decrease in TOP1 levels leads to RNA Pol II accumulation and AID abundance at *Ig* genes (Maul et al., 2015). Thus, the deficiency of TOP1 or inhibition of its DNA nicking activity locally at *Ig* locus may lead to more negative supercoiling and thus provide more ssDNA substrate for AID and thereby facilitate SHM. Our findings using immunofluorescence studies (Fig. 5**A, B, D** and **E**), co-localization (Fig. 6**, S7, S8** and **S9**) as well as proximity ligation assay experiments (Fig. 7**, S10, S11, S12** and **S13**) strongly suggest that similar to SRSF1, SRSF1-3 interacts with TOP1, which probably influences its activity via either sequestration or by inhibiting DNA nicking activity locally at the *Ig* locus, and thus can assists in the process of SHM. Previous reports showed that the RS domain of SRSF1 is not required for interaction with TOP1 and inhibition of its nicking activity (Kowalska-Loth et al., 2005), also supporting the notion that SRSF1-3, which does not have the RS domain, can still interact TOP1 and inhibit its activity. Our co-immunoprecipitation studies also showed that SRSF1-3 interacts with AID in chicken DT40-ASF cells (Fig. 5**F** and **G**), confirming the earlier reports of similar interaction in human 293 T cells (Kawaguchi et al., 2017). Thus, SRSF1-3 is interacting with a key SHM regulator, TOP1, as well as AID itself. The cross-talk between SRSF1-3, AID and TOP1 locally at the *Ig* locus might play a crucial role in SHM (Fig. 8).

4. Materials and methods

4.1. DT40-ASF chicken B-cell culture

DT40-ASF cells, a kind gift from Prof. James L Manley, Columbia University, USA, were cultured in RPMI 1640 medium (Invitrogen) supplement with 10% FBS (Invitrogen), 1% chicken serum (HiMedia), 50 μM 2-mercaptoethanol (Sigma Aldrich), 2 mM glutamine, 100 μg/ml penicillin G, and 50 μg/ml streptomycin (Invitrogen) at 39.5 °C in 5% CO_2.

4.2. Immunofluorescence studies

For the immunofluorescence studies, 5×10^6 DT40-ASF cultured cells were fixed in 4% paraformaldehyde (MP Biomedicals) for 20 min and permeabilized with PBS-T (0.05% Triton-X in PBS) for 20 min. Further, the cells were blocked for 30 minutes in PBS-T containing 5% BSA (Sigma Aldrich) and incubated with the primary antibody, either anti-SRSF1 or anti-FLAG (Table **S1**), (1:100) for 1 hour in PBS containing 2.5% BSA, followed by washing of cells in PBS-T for three times for 10 min each, and were incubated with the secondary antibody, either anti-mouse Alexa flour 488 or Alexa flour 594 (Table **S1**) (1:200) in PBS-T containing 2.5% BSA for 60 min. Subsequently, cells were washed thrice in PBS-T for 10 minutes each. Finally, high-resolution images were taken at 40 X magnifications using a confocal laser scanning microscope (Olympus, FV1200MPE). Mean fluorescent intensities were calculated by Image J software using intden and raw intden values.

4.3. Co-Immunoprecipitation of FLAG-tagged SRSF1-3

SRSF1-3 protein was immunoprecipitated using the anti-FLAG M2 magnetic beads (Sigma Aldrich) (Table **S1**) from SRSF1-3 reconstituted clones as well as the SRSF1-3 deficient control cells. 3×10^7 transfected DT40-ASF cultured cells were washed in PBS, centrifuged at 1100 rpm, 4 °C for 5 min. The cells were lysed in 50 mM Tris-Cl, pH-7.5, with 150 mM NaCl, 1 mM EDTA, 1% Triton-X 100 and Protease inhibitor + DNaseI, 1 μg/ml. Beads were separately equilibrated in TBS buffer (50 mM Tris-Cl, pH-7.5, with 150 mM NaCl). Cell lysates were incubated with anti-FLAG M2 magnetic beads for overnight at 4 °C on the shaker. Subsequently, the FLAG-tagged SRSF1-3 protein was

immunoprecipitated by using a magnetic separator (Sigma Aldrich). Finally, SRSF1-3 and its interacting proteins were eluted with 3X FLAG peptide (Apex Bio) and 0.1 M Glycine HCl, pH-3.0.

4.4. Silver staining of SDS PAGE gels

Co-immunoprecipitation of FLAG-tagged SRSF1-3 were analyzed on 12% SDS-PAGE gel and visualized by silver staining. Initially, the gels were fixed in 50% methanol, 12% glacial acetic acid, 0.05% formalin for overnight, washed for 3 times with 35% ethanol for 20 min each, sensitized with 0.02% $Na_2S_2O_3$ for 2 min and washed for 3 times with H_2O for 5 min each. Subsequently, the gels were stained with 0.2% $AgNO_3$, 0.076% formalin for 20 min in dark and washed for 3 times with H_2O for 2 min each. Finally, the gels were developed with 6% Na_2CO_3, 0.05% formalin, 0.0004% $Na_2S_2O_3$ and reactions were stopped with 1.46% EDTA for 5 min.

4.5. Co-immunoprecipitation of TOP1 and AID

Mouse anti-AID mAB (Invitrogen), rabbit anti-TOP1 pAB (Sigma Aldrich) forms complex with Protein-A agarose beads (Santa Cruz Biotechnology) and were used to co- immunoprecipitate AID and TOP1 protein from the whole cell lysate or nuclear extracts of SRSF1-3 reconstituted clones and the SRSF1-3 deficient control cells. Cells were lysed in a buffer containing 50 mM Tris-Cl, pH-8.0, 150 mM NaCl, 1.0% NP-40, and Protease inhibitor + 1 μg/ml DNaseI. Further, cell lysate was passed through 22 gauge needle multiple times to shear the DNA.

For Co-IP from the nuclear lysate, cells were rinsed three times with 1X PBS plus protease inhibitor and resuspended in Lysis Buffer 1 (50 mM Tris-Cl pH-7.5, 140 mM NaCl, 1 mM EDTA, 10% glycerol, 0.5% NP-40 and 0.25% Triton X-100), rocked for 10 min at 4 °C to isolate nuclei. Samples were centrifuged at 1,350 × *g* and pellets were washed with Lysis Buffer 2 (10 mM Tris-Cl, pH-8.0, 200 mM NaCl, 1 mM EDTA, and 0.5 mM EGTA) by gently rocking for 5 min at room temperature. Nuclei was resuspended in Lysis Buffer 3 (10 mM Tris-Cl, pH-8.0, 100 mM NaCl, 1 mM EDTA, 0.5 mM EGTA, and 0.5% N-lauroylsarcosine) and incubated on ice for 10 min.

Lysate supernatants were incubated with either anti-AID mAB or anti-TOP1 pAB antibody (5:500 dilutions) (**Table S1**) for overnight at 4 °C on a rota-spin. Afterwards, Protein-A agarose beads were washed and equilibrated in 1 ml of equilibration buffer (20 mM Tris-Cl pH-8.0, 5 mM $MgCl_2$, 5 mM $MnCl_2$, 150 mM NaCl and 1.0% NP-40). Samples were incubated with 20 μl slurry of protein-A on a rota-spin for 2 hrs at 4 °C and pelleted by centrifugation (2000 g, 3 min). Subsequently, pellets were washed three times in 1 ml of ice-cold washing buffer (20 mM Tris-Cl pH-8.0, 5 mM $MgCl_2$, 5 mM $MnCl_2$, 750 mM NaCl and 1.0% NP-40) with 5 min incubations between spins. Finally, the immunoprecipitated proteins were eluted with 100 μl of antibody strip buffer/elution buffer (120 mM Tris-Cl, pH 6.8, 1.0% SDS, at room temperature for 30 min on a shaker to elute the proteins) and boil the samples at 95 °C for 5 min.

4.6. Co-localization Assay

For the co-localization studies, 3×10^6 DT40 cells were washed with 1X PBS in 96 U bottom well plate (Corning) at 220 rcf, 4 °C for 5 min and fixed in 4% paraformaldehyde in 1X PBS (MP Biomedicals) for 20 min and permeabilized with PBS-T (0.05% Triton-X in PBS) for 20 min. Further, the cells were blocked for 30 minutes in PBS-T containing 5% BSA (Sigma Aldrich) and incubated with the primary antibody, namely, anti-mouse FLAG and anti-rabbit TOP1 (**Table S1**), (1:20) for overnight at 4 °C in 1X PBS containing 2.5% BSA, followed by washing of cells in PBS-T for three times for 10 min each, subsequently incubated with the secondary antibodies, anti-mouse Alexa flour 568 and anti-rabbit Alexa flour 488 (**Table S1**) (1:500) in PBS-T containing 2.5% BSA for 60 min at 4 °C in the dark. Subsequently, cells were washed thrice in PBS-T for 10 minutes each. DAPI with mounting medium (Genetex) was added to the wells and the cells were mounted on to the slides and these were kept at 37 °C for 60 min for drying. Finally, high-resolution images were taken at 60 X magnifications using a confocal laser scanning microscope (Olympus, FV3000).

4.7. Proximity ligation assay (PLA)

PLA was performed using reagents supplied in Duolink in situ Red PLA kit Mouse/Rabbit (Sigma-Aldrich, DUO92101), following the manufacturer's instructions. The protocol was first standardized so as to use a minimal volume of the probes and enzymes required for the reaction. Briefly, 3×10^6 DT40 cells were taken per well of a 96-well U-bottom plate and the protocol carried out for the co-localization studies, described previously, was followed. Subsequent to the primary antibodies incubation, overnight at 4 °C, cells were washed with wash buffer-A, twice at 220 rcf, 4 °C for 5 min each, followed by incubation with secondary antibodies conjugated to oligonucleotides (PLA Probes anti-mouse MINUS and PLA Probes anti-rabbit PLUS), diluted in antibody diluent (1:5) and incubated for 60 min at 37 °C in a humidity chamber. Cells were then washed twice with washing buffer-A, followed by centrifugation at 220 rcf at 4 °C for 5 min. The 5X ligation buffer was diluted in high purity water to a final concentration of 1X and the ligase (1U/μl) diluted 1:40 in the 1X ligation buffer. 20 μl of ligation mixture was added to each well and incubated for 30 min at 37 °C in the humidity chamber. Again, the cells were washed twice with washing buffer-A, followed by centrifugation at 220 rcf at 4 °C for 5 min. Further, 20 μl of amplification polymerase mixture (0.5 μl polymerase in 39.5 μl 1X amplification buffer, 1:80 dilution) was added to each well and incubated for 120 min at 37 °C in the humidity chamber. Cells were then washed twice with washing buffer-B at 220 rcf, 4 °C for 10 min and the final wash was with 0.01X washing buffer-B for 1 min. DAPI with mounting medium was added to the wells and the cells were mounted on to the slides. Slides were let to dry overnight at 4 C, scanned and images were acquired using a confocal laser scanning microscope (Olympus, FV1200MPE). Statistical analysis was performed by calculating the percentage of cells showing positive PLA signals. P-values were calculated using two-tailed Fishers t-test.

Author contributions

P. Kodgire and A. K. Singh designed the experiments; A. K. Singh, A. Tamrakar, and A. Jaiswal performed the experiments; N. Kanayama provided pCI-FLAG-SRSF1-3-bsr construct; A. Agarwal and P. Tripathi provided resources for co-localization and PLA studies. A. K. Singh and P. Kodgire wrote the manuscript.

Funding sources

No competing financial interests have been declared. Funding for this work was provided by Department of Science and Technology, Govt. of India, for research grants (EMR/2016/003547), (SR/S2/RJN-109/2011) and Department of Biotechnology, Govt. of India, for a research grant (BT/PR20319/BBE/117/189/2016).

Declaration of Competing Interest

The authors declare no competing interests.

Acknowledgements

Authors thank Prof. J. L. Manley, Columbia University, USA, for a kind gift of DT40-ASF cells. We thank Dr. S. Shukla, IISER Bhopal, India, for Histone H3 antibody. A. K. Singh, A. Tamrakar, and A. Jaiswal thank Department of Science and Technology (DST), University Grants Commission (UGC) and Council of Scientific and Industrial

Research (CSIR), Government of India, respectively, for PhD fellowship. A. Agarwal is supported by DST-WOS-A fellowship. Authors are thankful to Sophisticated Instrumentation Facility at IIT Indore and THSTI, Faridabad, for confocal experiments.

Appendix A. Supplementary data

Supplementary material related to this article can be found, in the online version, at doi:https://doi.org/10.1016/j.molimm.2019.10.002.

References

Baranello, L., Kouzine, F., Levens, D., 2013. DNA topoisomerases beyond the standard role. Transcription 4, 232–237.
Baranello, L., Wojtowicz, D., Cui, K., Devaiah, B.N., Chung, H.J., Chan-Salis, K.Y., Guha, R., Wilson, K., Zhang, X., Zhang, H., et al., 2016. RNA Polymerase II Regulates Topoisomerase 1 Activity to Favor Efficient Transcription. Cell 165, 357–371.
Caceres, J.F., Krainer, A.R., 1993. Functional analysis of pre-mRNA splicing factor SF2/ASF structural domains. EMBO J. 12, 4715–4726.
Caceres, J.F., Misteli, T., Screaton, G.R., Spector, D.L., Krainer, A.R., 1997. Role of the modular domains of SR proteins in subnuclear localization and alternative splicing specificity. J. Cell Biol. 138, 225–238.
Choudhary, M., Tamrakar, A., Singh, A.K., Jain, M., Jaiswal, A., Kodgire, P., 2018. AID Biology: A pathological and clinical perspective. Int. Rev. Immunol. 37, 37–56.
Conley, M.E., Dobbs, A.K., Farmer, D.M., Kilic, S., Paris, K., Grigoriadou, S., Coustan-Smith, E., Howard, V., Campana, D., 2009. Primary B cell immunodeficiencies: comparisons and contrasts. Annu. Rev. Immunol. 27, 199–227.
Conticello, S.G., Ganesh, K., Xue, K., Lu, M., Rada, C., Neuberger, M.S., 2008. Interaction between antibody-diversification enzyme AID and spliceosome-associated factor CTNNBL1. Mol. Cell 31, 474–484.
Ge, H., Zuo, P., Manley, J.L., 1991. Primary structure of the human splicing factor ASF reveals similarities with Drosophila regulators. Cell 66, 373–382.
Hagopian, J.C., Ma, C.T., Meade, B.R., Albuquerque, C.P., Ngo, J.C., Ghosh, G., Jennings, P.A., Fu, X.D., Adams, J.A., 2008. Adaptable molecular interactions guide phosphorylation of the SR protein ASF/SF2 by SRPK1. J. Mol. Biol. 382, 894–909.
Hu, Y., Ericsson, I., Doseth, B., Liabakk, N.B., Krokan, H.E., Kavli, B., 2014. Activation-induced cytidine deaminase (AID) is localized to subnuclear domains enriched in splicing factors. Exp. Cell Res. 322, 178–192.
Ishikawa, T., Krzysko, K.A., Kowalska-Loth, B., Skrajna, A.M., Czubaty, A., Girstun, A., Cieplak, M.K., Lesyng, B., Staron, K., 2012. Activities of topoisomerase I in its complex with SRSF1. Biochemistry 51, 1803–1816.
Kanehiro, Y., Todo, K., Negishi, M., Fukuoka, J., Gan, W., Hikasa, T., Kaga, Y., Takemoto, M., Magari, M., Li, X., et al., 2012. Activation-induced cytidine deaminase (AID)-dependent somatic hypermutation requires a splice isoform of the serine/arginine-rich (SR) protein SRSF1. Proc. Natl. Acad. Sci. U. S. A. 109, 1216–1221.
Kawaguchi, Y., Nariki, H., Kawamoto, N., Kanehiro, Y., Miyazaki, S., Suzuki, M., Magari, M., Tokumitsu, H., Kanayama, N., 2017. SRSF1-3 contributes to diversification of the immunoglobulin variable region gene by promoting accumulation of AID in the nucleus. Biochem. Biophys. Res. Commun. 485, 261–266.
Kobayashi, M., Sabouri, Z., Sabouri, S., Kitawaki, Y., Pommier, Y., Abe, T., Kiyonari, H., Honjo, T., 2011. Decrease in topoisomerase I is responsible for activation-induced cytidine deaminase (AID)-dependent somatic hypermutation. Proc. Natl. Acad. Sci. U. S. A. 108, 19305–19310.
Kodgire, P., Mukkawar, P., Ratnam, S., Martin, T.E., Storb, U., 2013. Changes in RNA polymerase II progression influence somatic hypermutation of Ig-related genes by AID. J. Exp. Med. 210, 1481–1492.
Kowalska-Loth, B., Girstun, A., Piekielko, A., Staron, K., 2002. SF2/ASF protein inhibits camptothecin-induced DNA cleavage by human topoisomerase I. Eur. J. Biochem. 269, 3504–3510.
Kowalska-Loth, B., Girstun, A., Trzcinska, A.M., Piekielko-Witkowska, A., Staron, K., 2005. SF2/ASF protein binds to the cap region of human topoisomerase I through two RRM domains. Biochem. Biophys. Res. Commun. 331, 398–403.
Leppard, J.B., Champoux, J.J., 2005. Human DNA topoisomerase I: relaxation, roles, and damage control. Chromosoma 114, 75–85.
Maul, R.W., Saribasak, H., Cao, Z., Gearhart, P.J., 2015. Topoisomerase I deficiency causes RNA polymerase II accumulation and increases AID abundance in immunoglobulin variable genes. DNA repair 30, 46–52.
Nguyen Ba, A.N., Pogoutse, A., Provart, N., Moses, A.M., 2009. NLStradamus: a simple Hidden Markov Model for nuclear localization signal prediction. BMC Bioinform. 10, 202.
Niu, D.K., Yang, Y.F., 2011. Why eukaryotic cells use introns to enhance gene expression: splicing reduces transcription-associated mutagenesis by inhibiting topoisomerase I cutting activity. Biol. Direct 6, 24.
Nowak, U., Matthews, A.J., Zheng, S., Chaudhuri, J., 2011. The splicing regulator PTBP2 interacts with the cytidine deaminase AID and promotes binding of AID to switch-region DNA. Nat. Immunol. 12, 160–166.
Pasqualucci, L., Bhagat, G., Jankovic, M., Compagno, M., Smith, P., Muramatsu, M., Honjo, T., Morse 3rd, H.C., Nussenzweig, M.C., Dalla-Favera, R., 2008. AID is required for germinal center-derived lymphomagenesis. Nat. Genet. 40, 108–112.
Pasqualucci, L., Neumeister, P., Goossens, T., Nanjangud, G., Chaganti, R.S., Kuppers, R., Dalla-Favera, R., 2001. Hypermutation of multiple proto-oncogenes in B-cell diffuse large-cell lymphomas. Nature 412, 341–346.
Peters, A., Storb, U., 1996. Somatic hypermutation of immunoglobulin genes is linked to transcription initiation. Immunity 4, 57–65.
Pommier, Y., 2006. srsfoisomerase I inhibitors: camptothecins and beyond. Nat. Rev. Cancer 6, 789–802.
Shen, H.M., Peters, A., Baron, B., Zhu, X., Storb, U., 1998. Mutation of BCL-6 gene in normal B cells by the process of somatic hypermutation of Ig genes. Science 1750–1752.
Shepard, P.J., Hertel, K.J., 2009. The SR protein family. Genome Biol. 10, 242.
Wang, J., Takagaki, Y., Manley, J.L., 1996. Targeted disruption of an essential vertebrate gene: ASF/SF2 is required for cell viability. Gene Dev. 10, 2588–2599.
Wang, X., Fan, M., Kalis, S., Wei, L., Scharff, M.D., 2014. A source of the single-stranded DNA substrate for activation-induced deaminase during somatic hypermutation. Nat. Commun. 5, 4137.
Yu, H., Droge, P., 2014. Replication-induced supercoiling: a neglected DNA transaction regulator? Trends Biochem. Sci. 39, 219–220.
Zhao, J., Bacolla, A., Wang, G., Vasquez, K.M., 2010. Non-B DNA structure-induced genetic instability and evolution. Cell Mol. Life Sci. 67, 43–62.
Zhu, J., Krainer, A.R., 2000. Pre-mRNA splicing in the absence of an SR protein RS domain. Genes Dev. 14, 3166–3178.
Zuo, P., Manley, J.L., 1993. Functional domains of the human splicing factor ASF/SF2. EMBO J 12, 4727–4737.